

2.1 Times Increase of Drain Efficiency by Dual Supply Voltage Scheme in 315MHz Class-F Power Amplifier at Output Power of -20dBm

Shunta Iguchi¹, Akira Saito², Kazunori Watanabe², Takayasu Sakurai¹, and Makoto Takamiya¹

¹University of Tokyo
Tokyo, Japan

²Semiconductor Technology Academic Research Center
Yokohama, Japan

Abstract—Dual power supply voltage (V_{DD}) scheme is proposed to increase the efficiency of a power amplifier (PA) with small output power (P_{OUT}) for short-range wireless sensor networks (e.g. body area networks). At P_{OUT} of -20dBm, compared with the conventional single V_{DD} PA, the drain efficiency (DE) and the global efficiency (GE) of the proposed dual V_{DD} PA increase by 2.1 times and 1.5 times, respectively. A class-F PA fabricated in 40-nm CMOS with the proposed dual V_{DD} (0.2V and 0.56V) achieves the highest DE of 42% at P_{OUT} of -20dBm in the published PA's. The PA is applied to a 315MHz OOK transmitter (TX) and the TX achieves the highest GE of 28% at P_{OUT} of -20dBm and the lowest energy of 36pJ/bit (= 36μW@1Mbps) in the published TX's.

I. INTRODUCTION

In short-range wireless sensor networks (e.g. body area networks), an ultra low power transmitter (TX) with small output power (P_{OUT}) is required. In this paper, the target P_{OUT} is -20dBm and the target communication distance is 1m, assuming -25dB propagation loss at the 1-m distance, -5dB x 2 loss at TX/RX antennas, and -55dBm receiver sensitivity [1]. The target TX power consumption (P_{TOTAL}) is less than 50μW at 1Mbps and 315-MHz carrier frequency. In order to reduce P_{TOTAL} of TX less than 50μW at P_{OUT} of -20dBm (= 10μW), the global efficiency (GE) ($= P_{OUT}/P_{TOTAL}$) of a TX should be larger than 20% ($= 10\mu\text{W}/50\mu\text{W}$). Increasing the efficiency at small P_{OUT} , however, is a design challenge.

Fig. 1 shows the dependence of drain efficiency (DE) on P_{OUT} in previously published power amplifiers (PA's) [1-7]. As P_{OUT} decreases, DE also decreases, because various losses become non-negligible. In PA's [4,5] for the conventional wireless communications (e.g. cell-phone and WLAN) where the communication distance is 100m~1km, P_{OUT} is +20dBm ~ +30dBm and DE is higher than 60%. In contrast, in PA's [1-3,7] for the short-range wireless sensor networks (e.g. body area networks) where the communication distance is 1m~10m, P_{OUT} is -20dBm ~ -10dBm and DE is less than 30%. For example, in our previous work [1], DE is 20% and GE is 16%, which does not meet our design target (GE > 20%). Therefore, the purpose of this paper is to achieve DE higher than 40% and GE higher than 20% at P_{OUT} of -20dBm. A newly proposed dual power supply voltage (V_{DD}) scheme increases DE and GE by 2.1 times and 1.5 times, respectively, compared with the conventional single V_{DD} scheme [1].

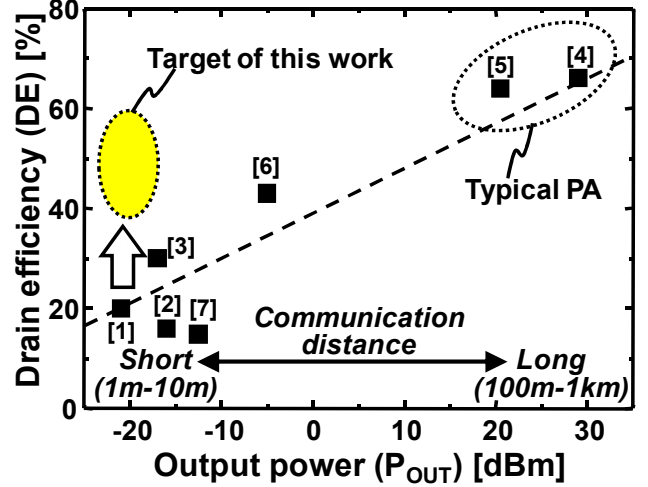


Fig. 1. Dependence of drain efficiency on output power in previously published PA's and target of this work.

II. DESIGN OF DUAL V_{DD} CLASS-F POWER AMPLIFIER

In this section, the dual V_{DD} scheme is introduced to increase DE of PA at P_{OUT} of -20dBm. In this paper, a class-F PA instead of a class-D or class-E PA is used, because the class-F PA achieved the highest efficiency at our design target.

Fig. 2 (a) shows a schematic of the class-F PA. V_{DD1} is the amplitude of the input (In) and V_{DD2} is the power supply voltage of PA. L_{DC} is a choke coil, C_{DC} is an AC-coupling capacitor, L_1 and C_1 resonate at the fundamental frequency (= 315MHz), and L_3 and C_3 resonate at the third harmonic (= 3 x 315MHz). Fig. 2 (b) shows an equivalent circuit of Fig. 2 (a) [8]. A transformer is formed by the L and C networks in Fig. 2 (a) equivalently. The transformer ratio is defined as n. P_{OUT} of the class-F PA in Fig. 2 (b) is given by [9]

$$P_{OUT} = \frac{\left(\frac{4}{\pi} \times V_{DD2} \right)^2}{2n^2 \times 50(\Omega)} \propto \left(\frac{V_{DD2}}{n} \right)^2. \quad (1)$$

Fig. 3 shows a dependence of P_{OUT} on V_{DD2} calculated with Eq. (1), when n is varied from 0.01 to 100. DE is the highest at n = 1, because the loss of the transformer in Fig. 2 (b) is proportional to n ($n > 1$) or $1/n$ ($n < 1$) [9]. Therefore, a PA design with n = 1 is the best design. The PA design with

P_{OUT} of -20dBm in this work is quite different from the typical PA design with P_{OUT} of +20dBm ~ +30dBm. In the latter design, n is less than 1, while n is larger than 1 in the former design. In order to increase DE in the typical PA, $V_{\text{DD}2}$ should be increased and n should be increased to 1. In contrast, in order to increase DE in the PA with P_{OUT} of -20dBm in this work, $V_{\text{DD}2}$ should be decreased and n should be decreased to 1. In the conventional PA's with small P_{OUT} [2, 3], however, $V_{\text{DD}2}$ is not decreased (-1V) and large n is used, thereby DE is reduced. In this work, $V_{\text{DD}2}$ is decreased to 0.2V and n is decreased to 4.2, which will be shown in Fig. 5 (b). If $V_{\text{DD}1}$ is also decreased to 0.2V, the on-current of the transistor in Fig. 2 (a) is greatly reduced, because the transistor operates in the sub-threshold region. In order to solve the problem, the dual V_{DD} scheme is proposed in this paper.

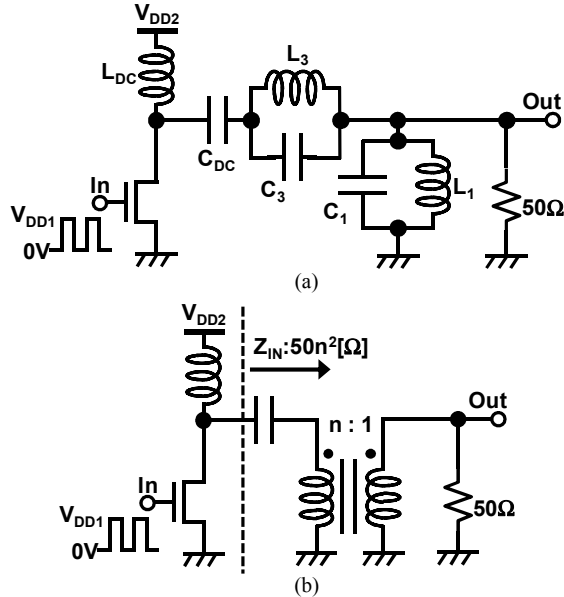


Fig. 2. (a) Schematic of a class-F PA. (b) Equivalent circuit of (a).

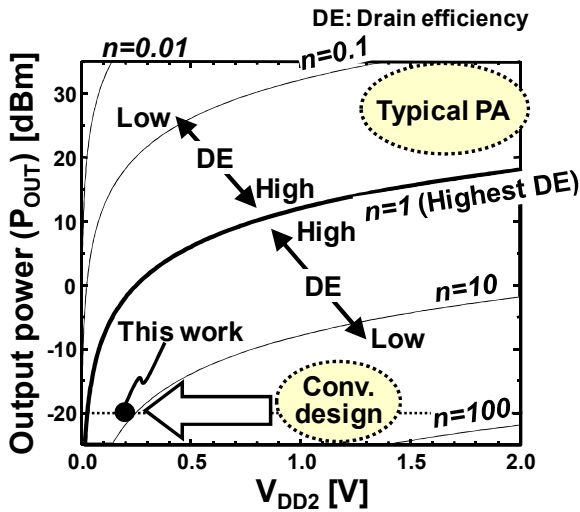


Fig. 3. Dependence of output power on $V_{\text{DD}2}$ calculated with Eq. (1). Transformer ratio (n) in Fig. 2 (b) is varied from 0.01 to 100.

III. DESIGN OF TRANSMITTER WITH DUAL V_{DD} POWER AMPLIFIER

In this section, the dual V_{DD} scheme is optimized to maximize GE of TX at P_{OUT} of -20dBm. Fig. 4 shows a schematic of TX including the dual V_{DD} class-F PA. The carrier frequency is 315MHz for a radio communication standard of ARIB STD-T93 (315MHz band) in Japan and the data rate is 1Mbps. As shown in Fig. 4, P_{TOTAL} is the sum of the buffer, the mixer, and the PA powers. In the PA design with P_{OUT} of -20dBm, the buffer power is not negligible and the PA-only (=DE only) design optimization is inadequate. Therefore, GE is maximized at P_{OUT} of -20dBm by optimizing n . In the design optimization, $V_{\text{DD}1}$, $V_{\text{DD}2}$, C_{DC} , and L_{DC} are varied according to n , and L_1 , C_1 , L_3 , C_3 , and transistor size are fixed.

Figs. 5 (a), (b), and (c) show the SPICE simulated n dependence in TX with P_{OUT} of -20dBm. Fig. 5 (a) shows the simulated dependence of P_{TOTAL} , the buffer power, and the PA power on n . Fig. 5 (b) shows the simulated dependence of $V_{\text{DD}1}$ and $V_{\text{DD}2}$ on n . Fig. 5 (c) shows the simulated dependence of C_{DC} and L_{DC} on n . C_{DC} and L_{DC} are decided by n and the impedance matching. The power consumption in Fig. 5 (a) is simulated at $V_{\text{DD}1}$ and $V_{\text{DD}2}$ shown in Fig. 5 (b) and C_{DC} and L_{DC} shown in Fig. 5 (c). As shown in Fig. 5 (b), the conventional TX with single V_{DD} is designed at $n = 9.6$ and $V_{\text{DD}1} = V_{\text{DD}2} = 0.47\text{V}$. In contrast, as shown in Fig. 5 (a), P_{TOTAL} is minimum at $n = 4.2$, thereby GE is maximum at $n = 4.2$. The corresponding $V_{\text{DD}1} = 0.56\text{V}$ and $V_{\text{DD}2} = 0.2\text{V}$. Table I shows the optimum parameters in the conventional single V_{DD} design and the dual V_{DD} design.

The reason for the optimum dual V_{DD} is discussed. When n is reduced from 10 to 2, $V_{\text{DD}2}$ is reduced (Fig. 5 (b)) and the PA power is reduced (Fig. 5 (a)). In contrast, $V_{\text{DD}1}$ is increased (Fig. 5 (b)) and the buffer power is increased (Fig. 5 (a)). When n is reduced below 3, $V_{\text{DD}1}$ drastically increases (Fig. 5 (b)), because the transistor operation changes from the saturation region to the linear region, thereby the corresponding buffer power drastically increases (Fig. 5 (a)). Therefore, P_{TOTAL} is minimum at $n = 4.2$ (Fig. 5 (a)), thereby GE is maximum at $n = 4.2$.

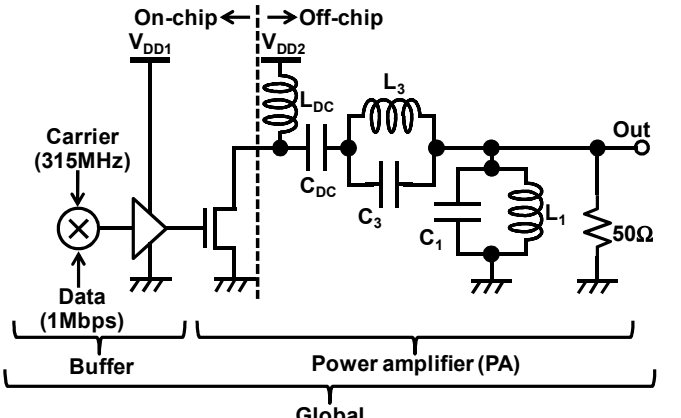


Fig. 4. Schematic of a dual V_{DD} TX with a class-F PA.

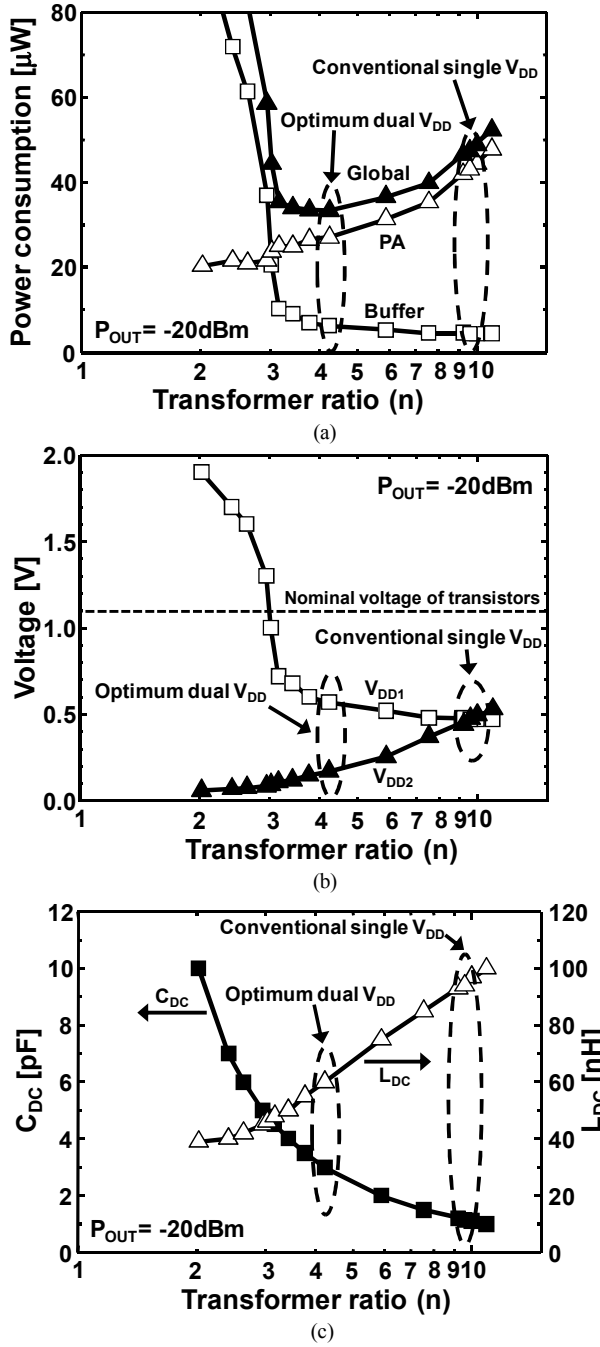


Fig. 5. SPICE simulated transformer ratio (n) dependence in TX with P_{OUT} of -20dBm . (a) Power consumption vs. n. (b) $V_{\text{DD}1}$ and $V_{\text{DD}2}$ vs. n. (c) C_{DC} and L_{DC} vs. n.

TABLE I PARAMETERS IN CONVENTIONAL SINGLE V_{DD} DESIGN AND PROPOSED DUAL V_{DD} DESIGN.

| | Conventional single V_{DD} | Proposed dual V_{DD} |
|----------------------|-------------------------------------|-------------------------------|
| $V_{\text{DD}1}$ [V] | 0.47 | 0.56 |
| $V_{\text{DD}2}$ [V] | 0.47 | 0.2 |
| C_{DC} [pF] | 1 | 3 |
| L_{DC} [nH] | 100 | 60 |

IV. MEASUREMENT RESULTS

To demonstrate the advantage of the proposed dual V_{DD} scheme, a test chip is fabricated in 1.1V, 40-nm CMOS process. Fig. 6 shows the die microphotograph and the layout. The die size is 0.5mm x 0.6mm and the core area of TX is 56μm x 22μm. The measured parameters of the conventional and the proposed PAs are given in Table I, while the same two resonators are used as follows: $L_1 = 22\text{nH}$, $C_1 = 11\text{pF}$, $L_3 = 2.7\text{nH}$, and $C_3 = 12\text{pF}$.

Fig. 7 shows the measured GE and P_{OUT} of TX in the proposed dual V_{DD} scheme, when $V_{\text{DD}1}$ and $V_{\text{DD}2}$ are varied. At the target P_{OUT} of -20dBm , the maximum GE is 28% at $V_{\text{DD}1} = 0.56\text{V}$ and $V_{\text{DD}2} = 0.2\text{V}$, which consists with the simulated results in Fig. 5. As P_{OUT} increases from -20dBm to -10dBm , the optimum $V_{\text{DD}1}$ and $V_{\text{DD}2}$ also increase. When $V_{\text{DD}1}$ is below 0.52V, the buffer fails to work at the 315-MHz carrier frequency.

Fig. 8 shows the measured output spectrum of the TX. The 314MHz carrier is modulated by 1Mbps OOK. The measured P_{OUT} of -20dBm meets the radio communication standard of ARIB STD-T93 (315MHz band) which specifies the operating frequency of 312-315.25MHz in Japan.

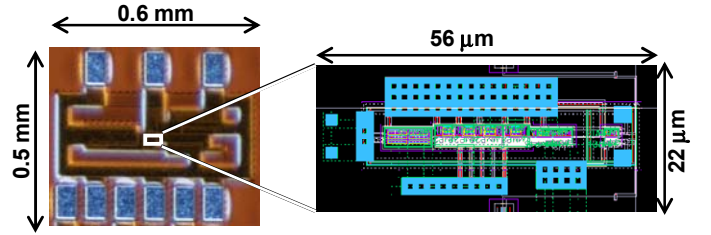


Fig. 6. Die microphotograph and layout of proposed dual V_{DD} PA in 40-nm CMOS.

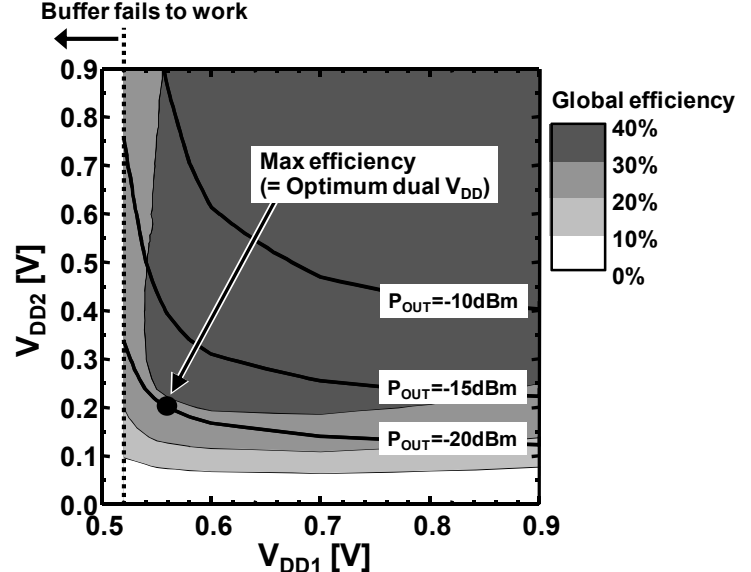


Fig. 7. Measured contours of global efficiency (GE) and P_{OUT} , when $V_{\text{DD}1}$ and $V_{\text{DD}2}$ are varied. Gray levels represent the values of GE. The lines are the contour of P_{OUT} . At target P_{OUT} of -20dBm , maximum GE is 28% at $V_{\text{DD}1} = 0.56\text{V}$ and $V_{\text{DD}2} = 0.2\text{V}$.

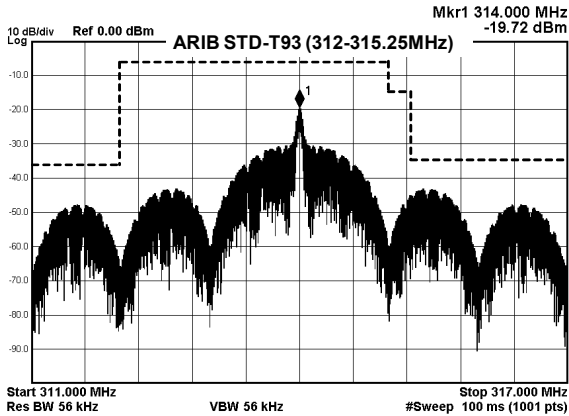


Fig. 8. Measured output spectrum of the TX. The 314MHz carrier is modulated by 1Mbps OOK.

Fig. 9 shows the measured dependence of DE and GE on P_{OUT} . The conventional single V_{DD} scheme and the proposed dual V_{DD} scheme are compared. In the single V_{DD} PA, $V_{\text{DD}1}$ and $V_{\text{DD}2}$ are varied with same value. In the dual V_{DD} PA, $V_{\text{DD}1}$ and $V_{\text{DD}2}$ are varied according to the optimum $V_{\text{DD}1}$ and $V_{\text{DD}2}$ in Fig. 7, respectively. At the target P_{OUT} of -20dBm, compared with the conventional single V_{DD} PA, DE and GE of the proposed dual V_{DD} PA increases by 2.1 times and 1.5 times, respectively.

The design issue of the proposed dual V_{DD} scheme is a DC-DC converter required for the additional V_{DD} . If the power conversion efficiency of the DC-DC converter is less than 66%, GE of the proposed dual V_{DD} PA with the DC-DC converter has no advantage over the conventional single V_{DD} PA. For example, however, a 0.45-V input buck converter with more than 90% efficiency from 2 μ W to 50 μ W [10] is reported. The proposed dual V_{DD} PA is still available with such converters.

In Fig. 9 and Table II, this work is compared with the previously published TX's with small P_{OUT} [1-3]. The proposed dual V_{DD} scheme achieves the highest DE of 42% and the highest GE of 28%, thereby achieving the lowest energy of 36pJ/bit (= 36 μ W@1Mbps) in the published TX's.

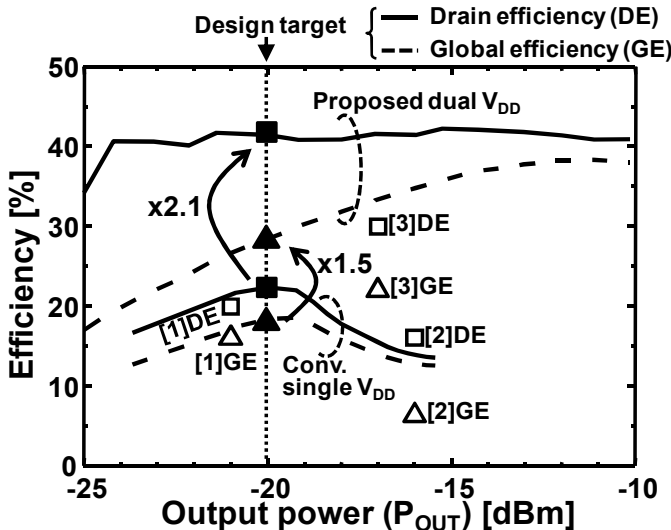


Fig. 9. Measured dependence of drain efficiency and global efficiency on output power. Conventional single V_{DD} PA and proposed dual V_{DD} PA are compared. Previous papers are also shown.

TABLE II COMPARISON WITH PREVIOUS PAPERS.

| | Unit | [2] | [3] | [1] | This work |
|---|---------|-------------------|-------------------|-----------------|---|
| CMOS technology | nm | 130 | 130 | 40 | 40 |
| Supply voltage | V | 1 | 1 | 0.5 | $V_{\text{DD}1}:0.56$ $V_{\text{DD}2}:0.2$ |
| Frequency | MHz | 300-450 | 400 | 315 | 315 |
| Data rate | Mbps | 0.1 | 0.2 | 1 | 1 |
| PA class | - | Edge-combiner | Edge-combiner | Class F | Class F |
| Output power (P_{OUT}) | dBm | -16 | -17 | -21 | -20 |
| Drain efficiency | % | 16 | 30 | 20 | 42 |
| Power consumption of TX (P_{TOTAL}) | μ W | 400 | 90 | 52 | 36 |
| Global efficiency ($P_{\text{OUT}}/P_{\text{TOTAL}}$) | % | 6.3 | 22 | 16 | 28 |
| Energy | pJ/bit | 4000 | 450 | 52 | 36 |
| TX includes | - | Osc.+PLL+Mixer+PA | Osc.+PLL+Mixer+PA | Mixer+Buffer+PA | Mixer+Buffer+PA |

V. CONCLUSIONS

The dual V_{DD} scheme is proposed to increase the efficiency of PA with small P_{OUT} . At P_{OUT} of -20dBm, compared with the conventional single V_{DD} PA, DE and GE of the proposed dual V_{DD} PA increases by 2.1 times and 1.5 times, respectively. Compared with the previously published papers, the proposed dual V_{DD} PA achieves the highest DE of 42% and the highest GE of 28% at P_{OUT} of -20dBm, thereby achieving the lowest energy of 36pJ/bit (= 36 μ W@1Mbps) in the published TX's.

ACKNOWLEDGMENT

This work was carried out as a part of the Extremely Low Power (ELP) project supported by the Ministry of Economy, Trade and Industry (METI) and the New Energy and Industrial Technology Development Organization (NEDO).

REFERENCES

- [1] A. Saito, K. Honda, Y. Zheng, S. Iguchi, K. Watanabe, T. Sakurai, and M. Takamiya, "An all 0.5V, 1Mbps, 315MHz OOK transceiver with 38- μ W carrier-frequency-free intermittent sampling receiver and 52- μ W Class-F transmitter in 40-nm CMOS," IEEE Symposium on VLSI Circuits, pp. 38-39 June 2012.
- [2] S. Rai, J. Holleman, J. Pandey, F. Zhang, and B. Otis, "A 500 μ W neural tag with 2 μ Vrms AFE and frequency-multiplying MICS/ISM FSK transmitter," IEEE International Solid-State Circuits Conference, pp. 212-213, Feb. 2009.
- [3] J. Pandey and B. Otis, "A sub-100 μ W MICS/ISM band transmitter based on injection-locking and frequency multiplication," IEEE J. Solid-State Circuits, vol. 46, no. 5, pp. 1049-1058, May 2011.
- [4] J. Lindstrand, C. Bryant, M. Tormanen, and H. Sjoland, "A 1.6-2.6GHz 29dBm injection-locked power amplifier with 64% peak PAE in 65nm CMOS," European Solid-State Circuits Conference, pp. 299-302, Sept. 2011.
- [5] J. Fritzin, T. Sundstrom, T. Johansson, and A. Alvandpour, "Reliability study of a low-voltage class-E power amplifier in 130nm CMOS," IEEE International Symposium on Circuits and Systems, pp. 1907-1910, June 2010.
- [6] K. Natarajan, J. S. Walling, and D. J. Allstot, "A Class-C power amplifier/antenna interface for wireless sensor applications," IEEE Radio Frequency Integrated Circuits Symp., pp. 1-4, June 2011.
- [7] G. Papotto, F. Carrara, A. Finocchiaro, and G. Palmisano, "A 90nm CMOS 5Mb/s crystal-less RF transceiver for RF-powered WSN nodes," IEEE International Solid-State Circuits Conference, pp. 452-454, Feb. 2012.
- [8] B. Razavi, RF Microelectronics. Prentice-Hall, 1998.
- [9] P. Reynaert and M. Steyaert, RF Power Amplifiers for Mobile Communications. Springer, 2006.
- [10] X. Zhang, P. Chen, Y. Ryu, K. Ishida, Y. Okuma, K. Watanabe, T. Sakurai, and M. Takamiya, "A 0.45-V input on-chip gate boosted (OGB) buck converter in 40-nm CMOS with more than 90% efficiency in load range from 2 μ W to 50 μ W," IEEE Symposium on VLSI Circuits, 194-195, June 2012.